Model thermodynamics and the role of free-carrier energy at high temperatures: Nitrogen and boron pairing in diamond

R. M. MacLeod, S. W. Murray,* J. P. Goss, P. R. Briddon, and R. J. Eyre
School of Electrical, Electronic and Computer Engineering, Newcastle University, Newcastle upon Tyne NE1 7RU, United Kingdom

(Received 23 April 2009; published 14 August 2009)

The role of configurational, vibrational, and electrical terms in the temperature-dependent binding energy of impurity pairs at high temperatures is considered by use of the example of boron and nitrogen in diamond. To calculate the free binding energy, we have developed a formalism for quantification of the free carrier contribution to the free binding energy. For doping concentrations of 10^{18} cm^{-3}, N_2 is favored over isolated substitutional N for temperatures up to ~2600 K, and boron favors the isolated substitutional form above ~750 K. Comparing with typical experimental conditions for growth or heat treatment, we show that the calculations account for the different behavior observed for B and N. For boron, the electronic contribution is large at low concentrations at the temperature at which B_s is able to migrate and cannot be neglected.

DOI: 10.1103/PhysRevB.80.054106 PACS number(s): 61.72.Bb, 65.40.gd, 63.20.kp

I. INTRODUCTION

The role of chemical and structural defects in crystalline materials plays a central part in the engineering of electronic and optical devices. A substantial contribution is being made to the understanding of defects using computational modeling, and in particular quantum-chemical simulations. Quantitative determination of measured quantities such as structures, vibrational modes, electrical levels, hyperfine interaction, and other experimentally determined quantities are key to the assignment of atomistic structures. However, the focus of this paper lies in the use of modeling to determine energetics of binding and in particular the binding energy of defect complexes in solid solution.

Binding energies typically quoted are zero-temperature free-energy differences, often neglecting contributions from zero-point energy (ZPE). However, binding energies are highly temperature dependent and computational determination of the temperature dependence has been the focus of a number of studies over the past few years.[1–5]

The key quantity to be determined is the free binding energy, E^b, defined as

$$E^b = F_{\text{dissociated}} - F_{\text{pair}}. \tag{1}$$

Then, a positive value for E^b indicates that impurity-pair formation is thermodynamically favored. In addition, we define a temperature T_0, such that $E^b(T_0)=0$. Previous calculations have been performed to determine the free binding energies of acceptor-oxygen complexes in Si.[3] Here, the free binding energy is

$$E^b = \Delta U + \Delta F_{\text{vib}} + \Delta F_{\text{elec}} - T\Delta S_{\text{config}}, \tag{2}$$

where ΔU is the difference in the zero-temperature Helmholtz free energy excluding ZPE, obtained from

$$\Delta U = 2E_{\text{isolated}} - E_{\text{pair}} - E_{\text{bulk}}, \tag{3}$$

where E_X is the total energy obtained using the density-functional method. ΔF_{vib} is the difference in vibrational free energy, ΔS_{config} is the difference in configurational entropy, and ΔF_{elec} is the free-carrier contribution. These terms are evaluated separately as detailed below. In previous calculations the contribution from the electrical term has been either assumed to be or shown to be small.[2]

However, for materials where processes occur at high temperatures, or where the electrical characteristics of the species when in complexes differs qualitatively from the dissociated component, it is not obvious that neglecting ΔF_{elec} is appropriate. To address this question, we present in detail the analysis for a representative problem in diamond, where impurity diffusion processes occur well above 1000 K. We also briefly outline the case for ΔF_{elec} for donor-vacancy complexes in silicon where the donor levels of the isolated donors are very shallow, whereas the electrical levels of the complexes are very deep.

A. Impurity pairs in diamond

Diamond, a wide-gap electrical insulator, may contain impurities introduced during growth. Many geological specimens contain nitrogen (termed[6] type-I diamond), often appearing in aggregated form (type Ia). A common form of aggregate, labeled the A center, consists of nitrogen substituting at neighboring host sites, shown schematically in Fig. 1(a). The nitrogen atoms relax away from each other, rendering them threefold coordinated. As all atoms have their valence satisfied, A centers are very deep donors: experimentally[7] and theoretically[8] at E_v+1.7 eV and E_v+1.8 eV, respectively, where E_v is the energy of the valence-band top.

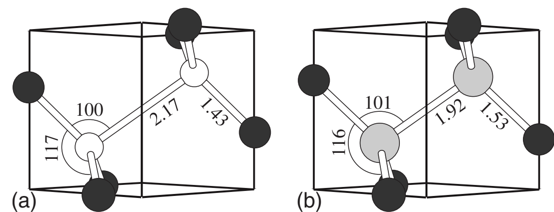

FIG. 1. Schematics of (a) N_2 and (b) B_2 in diamond, showing the impurities and their six equivalent neighbors. Bond lengths and angles are in Å and degrees, respectively. Dark and light gray, and white atoms are C, B, and N, respectively, with the boxes aligned along the cubic crystal axes.

 ©2009 The American Physical Society

In synthetic and rare natural diamonds, nitrogen occurs as isolated substitutional impurities (N_s). N_s has a donor level high in the band gap ($E_c-1.7$ eV),[9] associated with the formation of a neighboring carbon radical. Such diamond can be transformed into type Ia by annealing at high temperatures under a stabilizing pressure; analysis of experiments suggests aggregation is activated by around 5 eV,[10,11] and all N_s are converted into N_2 when N_s becomes mobile.

First-principles calculations estimate the binding energy of A centers relative to two separated N_s centers at 4 eV,[12,13] so once formed one expects N_2 be stable to high temperature. Indeed, aggregation of A centers into B centers (a lattice vacancy surrounded by nitrogen) requires annealing at 2500 K.[11]

In contrast, substitutional boron (B_s) theoretically undergoes a modest structural distortion, if any,[14–17] and results in a *relatively* shallow acceptor level ($E_v+0.37$ eV).[18] There is some evidence for the formation of boron substitutional dimers: the existence of a deep trap for hydrogen[19] and the correlation with a vibrational band[20,21] around 500 cm^{-1} which matches the vibrational modes predicted by first-principles modeling of these centers.[16,21] Boron dimers, such as the A centers, relax to form an extended "bond" between the two impurities. For B_2 this results from the depletion of electron density in this region, producing a deep acceptor level[8,16,19,21,22] estimated to lie 1–2 eV above E_v. A second acceptor level is even deeper.[19]

The binding energy of B_2 is much smaller than that of N_2; we previously reported values of 0.7–0.8 eV,[16,19] and other calculations support a small value.[21] Experimental efforts to aggregate boron by high-temperature annealing have led to little or no reduction in the concentration of acceptors.[23] Moreover, B doping can be achieved by indiffusion at high temperature.[24,25] Since this yields *p*-type diamond under indiffusion conditions where B_s is mobile, B appears to adopt the B_s form rather than B_2, which is in stark contrast to the efficient A-center formation in N-doped material when N_s becomes mobile.

In this paper we report the analysis of the temperature-dependent binding energy of boron and nitrogen pairs in diamond and also comment upon the contribution of ΔF_{elec} in the binding energy of E centers in silicon. We first present an outline of the method in Sec. II.

II. METHOD

A. First-principles modeling

Total-energy calculations are carried out using the local-spin-density-functional technique, implemented in AIMPRO.[26,27] To model the defects, 64 and 216 atom, cubic supercells of side length $2a_0$ and $3a_0$ were used. The Brillouin zone is sampled using the Monkhorst-Pack scheme[28] with a mesh of $2\times2\times2$ special k points. Core electrons are eliminated by using norm-conserving, separable pseudopotentials.[29]

The wave-function basis consists of atom-centered Gaussians.[30] Carbon atoms are treated using linear combinations of s and p orbitals with the addition of d functions to allow for polarization, totaling 13 functions per atom. Nitrogen and boron are treated using independent sets s and p Gaussians with four widths, respectively, with the addition of two and one sets of d-polarization functions for the N and B atoms, respectively. The charge density is Fourier transformed using plane waves with a cut off of 350 Ry, yielding well converged total energies.

This procedure yields lattice constant and bulk modulus of bulk diamond to within ~1% and 5%, respectively, of experiment, while the direct and indirect band gaps at 5.68 and 4.26 eV, respectively, are close to previously published plane-wave values.[31]

B. Vibrational free energy

ΔF_{vib} arises from differences in the vibrational properties of the paired and isolated configurations. Vibrational modes are obtained from the first-principles model by constructing the dynamical matrix using calculated second derivatives of the total energy with respect to position for all atoms in the 64 atom supercell and diagonalizing in the usual way. This was carried out for each of the configurations of interest, including bulk diamond.

The harmonic-approximation contribution to the vibrational free energy of each system is obtained using[2]

$$F_{\text{vib}}(T) = k_B T \int_0^\infty \{\ln[\sinh(h\omega/4\pi k_B T)]\} g(\omega) d\omega, \quad (4)$$

where k_B is Boltzmann's constant, T is absolute temperature, h is Plank's constant, and $g(\omega)$ is the vibrational density of states. The integral over $g(\omega)$ can be approximated by a sum over the zone-center normal modes of a large supercell. The ZPE per atom of bulk diamond obtained using our approximations is evaluated to be 0.183 eV, which compares very favorably with the value of 0.188 eV reported previously.[2]

C. Configurational entropy

Configurational entropy may be written $S=k_B \ln \Omega$, where Ω is the number of configurations, so the configurational term in Eq. (2) is

$$\Delta S_{\text{config}} = k_B \ln(\Omega_{\text{dissociated}}/\Omega_{\text{pairs}}). \quad (5)$$

For M impurities, the number of configurations can be expressed using combinatorial principles as

$$\Omega_{\text{dissociated}} = 2^M 4^M \frac{N!}{(N-M)!\,M!}, \quad (6)$$

where N is the number of host sites. The 2^M and 4^M terms account for the random effective-spins and crystallographic orientations of each center, respectively.

Complete aggregation yields $M/2$ dimers. It can be shown that the number of arrangements of dimers is

$$\Omega_{\text{pairs}} = \frac{(2N)!}{(2N-M/2)!\,(M/2)!}. \quad (7)$$

This expression may be understood by considering the number of ways of choosing $M/2$ bonds since each impurity pair is associated with a unique host bond.

D. Free energy of free carriers

Previously,[2] electronic contributions to the free energy have been based upon Boltzmann statistics. Here we present a more detailed model for the electronic contribution to the free energy based upon textbook statistical thermodynamic principles.

The free-carrier contribution is most significant for systems with shallow electrical levels. Therefore, of the four defect systems investigated in this study, only B_s meets this criterion, having an acceptor level between E_v and $E_v+0.37$ eV, depending upon boron concentration. For low temperatures, classical Maxwell-Boltzmann statistics become increasingly inaccurate, prompting our use of Fermi-Dirac analysis, based on a free-electron model.

Initially, the electron chemical potential (μ_e) is determined by equating the number of holes in the valence band (n_h) with the number of ionized acceptors (n_e). This ignores the electrons excited into the conduction band the number of which is expected to be negligible.

$$n_\mathrm{e}(\mu_e) - n_\mathrm{h}(\mu_e) = 0. \tag{8}$$

The number of ionized holes per unit volume is given by

$$n_\mathrm{h} = \sum_{i=1}^{N} \int_{-\infty}^{E_i} \frac{1}{2\pi}\left(\frac{2m_i}{\hbar^2}\right)^{3/2} \frac{(E_i - E)^{1/2}}{1 + \mathrm{e}^{(\mu_e - E)/k_B T}} \mathrm{d}E, \tag{9}$$

where N is the number of valence bands, E_i is the band-edge energy, m_i is the band effective mass, and $\hbar = h/2\pi$. In diamond the split-off band at Γ lies 6 meV below the valence-band top, so we approximate it as being degenerate with the heavy and light hole bands. By defining the density-of-states valence-band effective mass, m_dh, all valence bands may be treated as a single band with mass

$$m_\mathrm{dh} = (m_\mathrm{hh}^{3/2} + m_\mathrm{lh}^{3/2} + m_\mathrm{so}^{3/2})^{2/3},$$

where subscripts refer to heavy and light hole bands and split-off band, respectively.

The defect-level density of states is approximated using a delta function. This model breaks down for extremely high doping concentrations where the boron-acceptor levels either combine into an impurity band or drop into the valence band. However, for moderate concentrations this approximation allows the expression for the number of electrons per unit volume ionized into the acceptor level to be greatly simplified

$$n_\mathrm{e}(\mu_e) = \frac{N_0}{V} \frac{1}{1 + \beta \mathrm{e}^{(E_\mathrm{a} - \mu_e)/k_B T}}, \tag{10}$$

where N_0 is the number of acceptors, V is the sample volume, and E_a is the acceptor level. The spin-degeneracy factor β, accounts for there being the same degeneracy of the acceptor level as there is at the valence-band edge. All of these acceptor states are localized, however, so only one electron (of either spin up or down) is able to occupy one of these states,[32] giving $\beta = 3 \times 2 = 6$ in this case. Equation (8) must be solved numerically to obtain μ_e. Subsequently the free-carrier energy and entropy can be evaluated using Eqs. (11) and (12),[33] respectively.

TABLE I. Configurational entropy (eV/K) per defect for dissociated and paired defects at impurity concentrations of 10^{18} cm^{-3} and 10^{20} cm^{-3}.

Configuration	10^{18} cm^{-3}	10^{20} cm^{-3}
Paired	6.2×10^{-4}	4.3×10^{-4}
Dissociated	1.3×10^{-3}	9.1×10^{-4}

For donor systems, it is a simple matter to replace the valence bands and acceptor levels with conduction bands and donor levels. In our calculations, a value of $m_\mathrm{dh} = 0.8\ m_\mathrm{e}$ was used, lying between experimental values[34,35] of 0.75 m_e and 0.88 m_e. There remains a great deal of uncertainty in the true value, so additional calculations were conducted using values of $m_\mathrm{dh} = 0.1\ m_\mathrm{e}$ and $m_\mathrm{dh} = 1.1\ m_\mathrm{e}$.[36] For the donor systems, the effective mass of conduction electrons was taken as $m_\mathrm{de} = 0.2\ m_\mathrm{e}$.[32]

$$U_\mathrm{elec} = \int_{-\infty}^{E_\mathrm{v}} \frac{1}{2\pi}\left(\frac{2m_\mathrm{dh}}{\hbar^2}\right)^{3/2} \frac{E(E - E_\mathrm{v})^{1/2}}{1 + \mathrm{e}^{(E - \mu_e)/k_B T}} \mathrm{d}E - \frac{N_0}{V} \frac{E_\mathrm{a}}{1 + \beta \mathrm{e}^{(E_\mathrm{a} - \mu_e)/k_B T}} \tag{11}$$

$$\begin{aligned} S_\mathrm{elec} = k_B \int_{-\infty}^{E_\mathrm{v}} \Bigg[& \frac{\ln(1 + \mathrm{e}^{(E - \mu_e)/k_B T})}{1 + \mathrm{e}^{(E - \mu_e)/k_B T}} \\ & + \frac{\ln(1 + \mathrm{e}^{(\mu_e - E)/k_B T})}{1 + \mathrm{e}^{(\mu_e - E)/k_B T}} \Bigg] \frac{1}{2\pi}\left(\frac{2m_\mathrm{dh}}{\hbar^2}\right)^{3/2} (E_i - E)^{1/2} \mathrm{d}E \\ & + k_B \frac{N_0}{V} [\ln(1 + \mathrm{e}^{E_\mathrm{a} - \mu_e})/k_B T) 1 + \mathrm{e}^{(E_\mathrm{a} - \mu_e)/k_B T} \\ & + \frac{\ln(1 + \mathrm{e}^{(\mu_e - E_\mathrm{a})/k_B T})}{1 + \mathrm{e}^{(\mu_e - E_\mathrm{a})/k_B T}} \frac{1}{1 + \beta \mathrm{e}^{(E_\mathrm{a} - \mu_e)/k_B T}}. \end{aligned} \tag{12}$$

III. RESULTS

Density functional simulations provide energies for the four configurations, yielding zero-temperature free binding energies of 1.0 and 3.8 eV for B and N pairs, respectively, of which 0.3 eV and -0.1 eV are contributions from ΔF_vib. To illustrate the temperature-dependent contributions to the free binding energy, we present details for two impurity concentrations; $[X] = 10^{18}$ cm^{-3} and $[X] = 10^{20}$ cm^{-3}, where X=N or B. The configurational entropies of the paired and dissociated defects, which are independent of X, obtained from Eqs. (7) and (6) are summarized in Table I.

A key parameter in the free-carrier contribution to the E_b is the B_s acceptor level. We have used values of $E_a = E_v + 0.37$ eV and $E_a = E_v + 0.20$ eV, respectively, for $[\mathrm{B}] = 10^{18}$ cm^{-3} and $[\mathrm{B}] = 10^{20}$ cm^{-3}, respectively, obtained using the Pearson-Bardeen expression[37] fitted to the data in Fig. 4 of Ref. 38. To assess the impact of the choice of acceptor level, calculations were repeated using upper and lower bounds on the experimental data, also fitted to the Pearson-Bardeen expression, as shown in Fig. 2. Results of

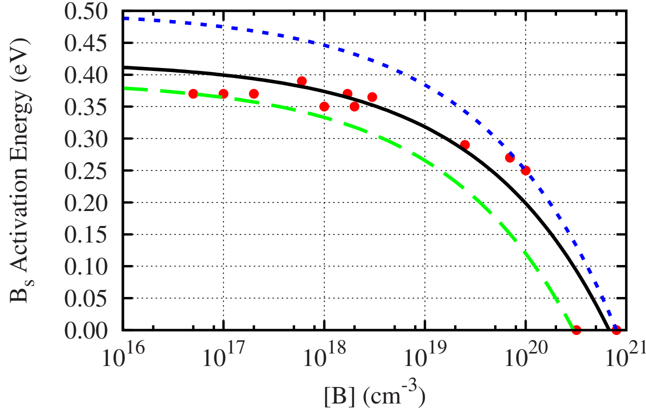

FIG. 2. (Color online) A plot of the B_s acceptor level relative to E_v (eV) vs [B] (cm^{-3}). Points show data from Fig. 4 of Ref. 38. The solid line shows the fitted Pearson-Bardeen profile, with dotted and dashed lines indicating the upper and lower bounds used as described in the text.

the analysis are presented in Table II, which summarizes the resulting changes in E^b, and T_0, with changes to m_{dh} and E_a. The impact of either the acceptor level or effective mass on the free binding energy is very modest within the specified bounds and the effect upon the critical temperature is correspondingly small with the possible exception of the high boron concentration and low hole effective mass. We conclude that uncertainties in these values are not likely to qualitatively affect any conclusions, as presented in Sec. IV.

Figure 3 shows the free binding energy and its three contributions as a function of temperature for $[N]=10^{18}$ cm^{-3} and $[N]=10^{20}$ cm^{-3}. As found in similar studies for different materials,[2,3,39] the configurational term is the largest term with the other terms being largely negligible. We obtain values of $T_0=2500$ K for $[N]=10^{18}$ cm^{-3} and $T_0=3500$ K for $[N]=10^{20}$ cm^{-3}, consistent with the stability of A centers relative to N_s.[11]

Similarly, Fig. 4 shows the contributions to the boron free binding energy. The configurational term again is the single largest contribution but those from ΔF_{vib} and ΔF_{elec} are more significant than in the nitrogen case. The contribution to T_0 from ΔF_{elec} lowers its value from 870 K to 800 K, for $[B]=10^{18}$ cm^{-3}, and from 1460 K to 1300 K for $[B]=10^{20}$ cm^{-3}, relative to where the electrical term is neglected. We shall return to this effect in Sec. IV.

TABLE II. The shifts in free binding energy, ΔE^b (meV), and critical temperature, ΔT_0 (K) when using extreme values for the density-of-states effective hole mass, m_{dh}, and acceptor level, E_a. Shifts are relative to the standard values used, i.e., $m_{dh}=0.8$ and the fitted value for E_a from Fig. 2, with E_a^{upper} and E_a^{lower} taken from the dashed and dotted curves, respectively.

	$[B]=10^{18}$ cm^{-3}		$[B]=10^{20}$ cm^{-3}	
	ΔE^b	ΔT_0	ΔE^b	ΔT_0
$m_{dh}=0.1$ m_e	70	70	110	170
$m_{dh}=1.1$ m_e	−20	−10	−30	−40
E_a^{lower}	−30	−20	−70	−80
E_a^{upper}	40	30	30	40

Finally we consider the boron in-diffusion experiments in the light of our calculations. Studies have been carried out at temperatures of 1400 °C (Ref. 24) and 1600 °C.[25] The relatively high temperatures are required for migration of B_s into the diamond (theoretically predicted[16] to be activated by 7.6 eV) but also will impact upon the equilibrium structure the boron will subsequently adopt. The former experiment estimated that a boron concentration of 3×10^{19} cm^{-3} had been obtained. At this concentration, our model predicts $T_0=1050$ K, so in equilibrium the conditions clearly favor the isolated substitutional acceptors, consistent with *p*-type material.

IV. DISCUSSION

We have calculated the free binding energies of boron and nitrogen substitutional pair defects in diamond. Contributions to the binding energy included the zero-temperature Helmholtz energy from a first-principles density-functional calculation, vibrational and configurational-entropic energies, and the free-energy contribution due to free carriers, which is found to be large for defects with shallow electrical

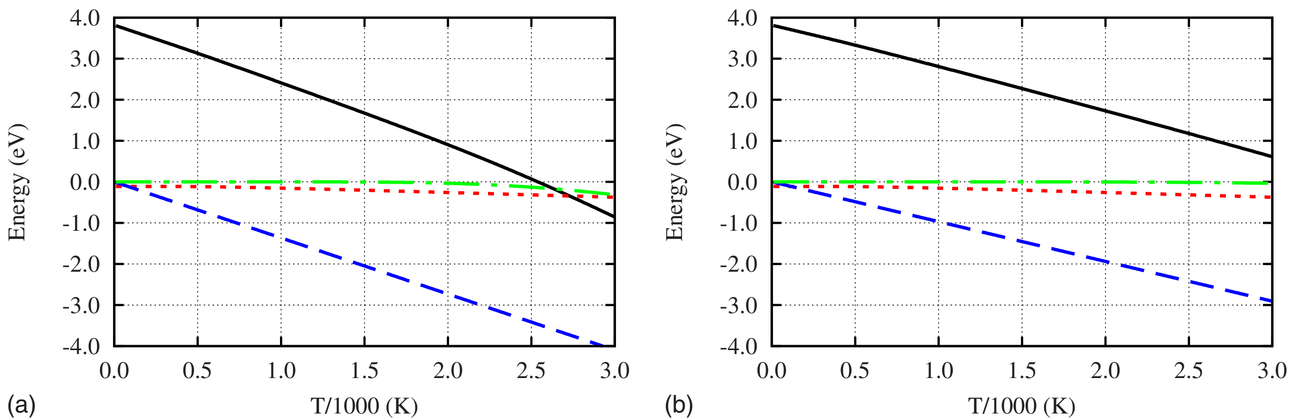

FIG. 3. (Color online) Components of the free binding energy of nearest-neighbor nitrogen pairs in diamond (eV). (a) $[N]=10^{18}$ cm^{-3} cm^{-3}. (b) $[N]=10^{20}$ cm^{-3}. The solid, dotted, dashed and dot-dashed lines show E^b, ΔF_{vib}, ΔF_{conf}, and ΔF_{elec}, respectively.

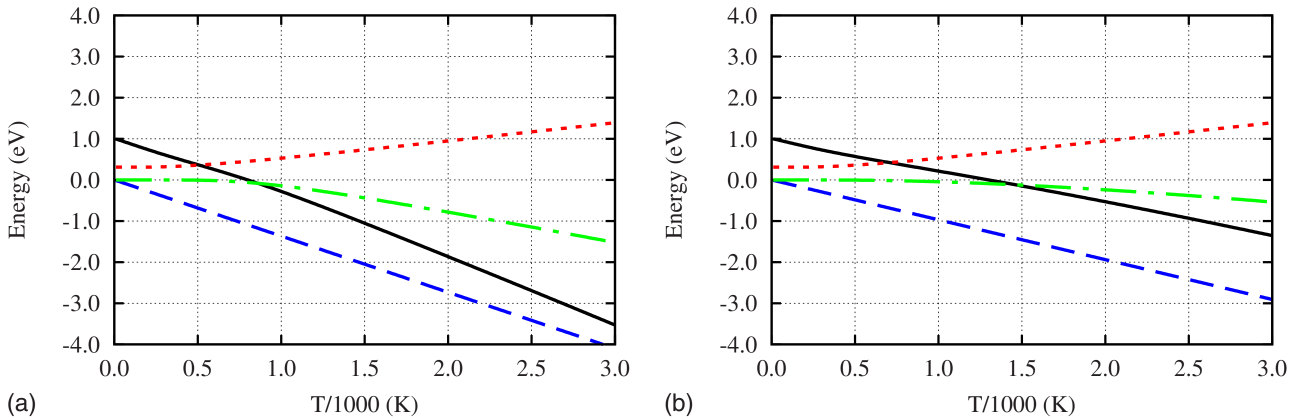

FIG. 4. (Color online) Components of the free binding energy between of nearest-neighbor boron impurity pairs (eV). (a) [B] $=10^{18}$ cm^{-3}. (b) [B]$=10^{20}$ cm^{-3}. Lines are as in Fig. 3.

levels. The last of these terms has been calculated in a more rigorous way than in previous studies.[2,3,39]

Figure 5 summarizes our results, showing the critical temperature where the binding energy of the pairs is zero, T_0, as a function of doping concentration for both chemical species. Below the main curve for each dopant species, the system will favor the paired configuration, and above will favor dissociation. Also shown are the curves for $T(E^b=\pm 0.2\ eV)$ indicating how rapidly the binding energy is varying.

The main conclusions we draw may be summarized as follows:

1. Substitutional nitrogen thermodynamically favors the N_2 configuration over N_s to high temperatures (1000 s of Kelvin) for even the lowest concentrations studied here in agreement with observed behavior of high-temperature annealing of N containing diamond. The fact that N_s is seen preferentially in synthetic material is a consequence of kinetic factors as the mobility of substitutional nitrogen is limited by a diffusion barrier of several eV.

2. Chemical vapor deposition of diamond, depending upon film type and substrate material occurs with a substrate temperature of $\sim$900–1400 K,[40,41] somewhat above the value of B_2 critical temperature of $T_0=760$ K when [B] $=10^{18}$ cm^{-3}. Our analysis suggest at 900 K at this concentration, the equilibrium ratio $[B_2]/[B_s]\approx 0.06$, with this ratio decreasing with increasing growth temperature. We note that if $\Delta F_{\rm elec}$ is not included in this calculation, this ratio is increased by an order of magnitude. Importantly, $\Delta F_{\rm vib}$ is more significant when compared to the configurational contribution than in systems previously analyzed.[2,3,39]

3. At the higher concentration of [B]$=10^{20}$ cm^{-3}, the value of T_0 is increased to 1200 K, consistent with B_2 being observed experimentally when higher concentrations are present,[20] although kinetic factors will also important. This temperature is also relatively close to that used for indiffusion experiments, and again, when analyzing such experiments, it is important to include the $\Delta F_{\rm elec}$ contribution.

In terms of the impurity pairs in diamond, we conclude that the model thermodynamics and statistical mechanics are able to explain the difference in aggregation behavior observed for N and B in diamond. Finally in terms of the boron and nitrogen pairs in diamond, we note that the $\Delta F_{\rm elec}$ term is most significant for light doping where the complex formation converts a shallow level to a deep one. In the current application this means that the role of $\Delta F_{\rm elec}$ is largest for boron pairs in the 10^{18} cm^{-3} case. To further explain the significance of the electrical term, its variation for boron is illustrated in Fig. 6. The change in slope in Fig. 6 around 1000 K reflects the impact of the deep acceptor level of B_2 at high temperatures: we used a value of E_v+1 eV for the purposes of this simulation,[16] but the contribution to $\Delta F_{\rm elec}$ is dominated by that of the B_s species, and the details of the B_2 acceptor level does not significantly affect this analysis. The important result is that for low concentrations and temperatures typical for boron migration, the contribution for the binding energy from the electrical term is of the same order as the zero-temperature binding energy, so that in this case the electronic term alone renders the pairs thermodynamically unbound during indiffusion.

As a final point, we consider the implications for defects in a narrow-gap material, silicon. The acceptor level of B_s in diamond is deep in comparison to typical doping levels in

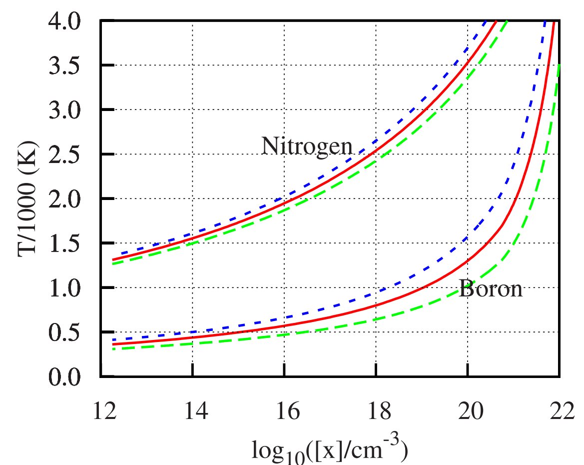

FIG. 5. (Color online) A plot of the calculated zero binding-energy critical temperature, T_0 (K), as a function of defect concentration for boron and nitrogen. The region where the pairs are unbound lies above the solid curves. Dotted and dashed lines indicate where $E^{\rm b}=0.2$ eV and $E^{\rm b}=-0.2$ eV, respectively.

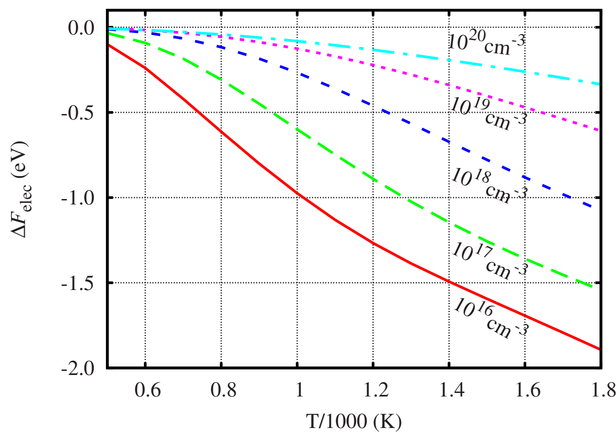

FIG. 6. (Color online) Graph of ΔF_{elec} for the boron pairs showing the variation with temperature for a range of boron concentrations as labeled.

electrically conductive semiconductors. In silicon substitutional phosphorus and arsenic have donor levels at 45 and 49 meV,[4,42] whereas complexes with a lattice vacancy have relatively deep levels.[43] Assuming that the ΔF_{elec} term in the temperature dependence of the binding energy for the As-V and P-V complexes in silicon is entirely associated with ionization of the phosphorus or arsenic donors, we can readily estimate its magnitude. At 420 K, the temperature where E centers begin to dissociate in experiment,[44,45] the contribution for concentrations of 10^{16}, 10^{17}, and 10^{18} cm^{-3} are estimated at −0.30, −0.22, and −0.14 eV, respectively.[46] We conclude that in this important case, the contribution of ΔF_{elec} is not obviously negligible, as at the lowest concentration considered here ΔF_{elec} is on the order of 30% of the zero-temperature binding energy.[47]

In summary, we have shown that model thermodynamics and statistical mechanics combined with first-principles calculations account for the stability of N pairs and relative lack of stability of boron pairs in diamond. Significant contributions to the temperature dependence of the binding energy can arise from the electrical contribution where the dissociated component has substantially different electrical levels from the complex, or vice versa, and we conclude that it is not generally true that the electrical term can be neglected in model thermodynamical simulations of defect processes.

---

*Present address: School of Mathematics, University of Edinburgh, Edinburgh, EH9 3JZ, UK.

[1] M. Sanati and S. K. Estreicher, Proceedings of the 22nd International Conference on Defects in Semiconductors (ICDS-22) University of Aarhus, Aarhus, Denmark July 28-August 1, 2003 [Physica B **340–342**, 630 (2003)].

[2] S. K. Estreicher, M. Sanati, D. West, and F. Ruymgaart, Phys. Rev. B **70**, 125209 (2004).

[3] M. Sanati and S. K. Estreicher, Phys. Rev. B **72**, 165206 (2005).

[4] S. M. Myers, A. F. Wright, M. Sanati, and S. K. Estreicher, J. Appl. Phys. **99**, 113506 (2006).

[5] T. Miyazaki and S. Yamasaki, Phys. Status Solidi A **202**, 2134 (2005).

[6] G. S. Woods, *Properties and Growth of Diamond*, EMIS Datareviews Series Vol. 9 (INSPEC, Institute of Electrical Engineers, London, 1994), Chap. 3.1, pp. 83–84.

[7] G. Davies, J. Phys. C **9**, L537 (1976).

[8] J. P. Goss, P. R. Briddon, R. Jones, and S. Sque, Proceedings of the 14th European Conference on Diamond, Diamond-Like Materials, Carbon Nanotubes, Nitrides and Silicon Carbide [Diamond Relat. Mater. **13**, 684 (2004)].

[9] R. G. Farrer, Solid State Commun. **7**, 685 (1969).

[10] T. Evans, Z. Qi, and J. Maguire, J. Phys. C **14**, L379 (1981).

[11] T. Evans and Z. Qi, Proc. R. Soc. London, Ser. A **381**, 159 (1982).

[12] T. Miyazaki, H. Okushi, and T. Uda, Phys. Rev. Lett. **88**, 066402 (2002).

[13] J. P. Goss, I. Hahn, R. Jones, P. R. Briddon, and S. Öberg, Phys. Rev. B **67**, 045206 (2003).

[14] S. J. Breuer and P. R. Briddon, Phys. Rev. B **49**, 10332 (1994).

[15] J. P. Goss, P. R. Briddon, M. J. Rayson, S. J. Sque, and R. Jones, Phys. Rev. B **72**, 035214 (2005).

[16] J. P. Goss and P. R. Briddon, Phys. Rev. B **73**, 085204 (2006).

[17] E. B. Lombardi, A. Mainwood, and K. Osuch, Phys. Rev. B **70**, 205201 (2004).

[18] P. A. Crowther and P. J. Dean, J. Phys. Chem. Solids **28**, 1115 (1967).

[19] J. P. Goss, P. R. Briddon, R. Jones, Z. Teukam, D. Ballutaud, F. Jomard, J. Chevallier, M. Bernard, and A. Deneuville, Phys. Rev. B **68**, 235209 (2003).

[20] M. Bernard, C. Baron, and A. Deneuville, Proceedings of the 14th European Conference on Diamond, Diamond-like Materials, Carbon Nanotubes, Nitrides and Silicon Carbide September 8–12, 2003, Salzburg, Austria [Diamond Relat. Mater. **13**, 896 (2004)].

[21] E. Bourgeois, E. Bustarret, P. Achatz, F. Omnés, and X. Blase, Phys. Rev. B **74**, 094509 (2006).

[22] Y. Cai, T. Zhang, A. B. Anderson, J. C. Angus, L. N. Kostadinov, and T. V. Albu, Proceedings of the 11th International Conference on New Diamond Science and Technology/9th Applied Diamond Conference May 15–19, 2006, Research Triangle Park, NC [Diamond Relat. Mater. **15**, 1868 (2006)].

[23] S. C. Lawson (private communication).

[24] W. Tsai, M. Delfino, D. Hodul, M. Riaziat, L. Y. Ching, G. Reynolds, and C. B. Cooper, IEEE Electron Device Lett. **12**, 157 (1991).

[25] O. B. Krutko, P. B. Kosel, R. L. C. Wu, S. J. Fries, S. Heidger, and J. Weimer, Appl. Phys. Lett. **76**, 849 (2000).

[26] R. Jones and P. R. Briddon, in *Identification of Defects in Semiconductors*, Semiconductors and Semimetals, Vol. 51A, edited by M. Stavola (Academic, Boston, 1998), Chap. 6.

[27] M. J. Rayson and P. R. Briddon, Comput. Phys. Commun. **178**, 128 (2008).

[28] H. J. Monkhorst and J. D. Pack, Phys. Rev. B **13**, 5188 (1976).

[29] C. Hartwigsen, S. Goedecker, and J. Hutter, Phys. Rev. B **58**, 3641 (1998).

[30] J. P. Goss, M. J. Shaw, and P. R. Briddon, in *Theory of Defects in Semiconductors*, Topics in Applied Physics, Vol. 104, edited by David A. Drabold and Stefan K. Estreicher (Springer, Berlin, 2007), pp. 69–94.
[31] D. A. Liberman, Phys. Rev. B **62**, 6851 (2000).
[32] S. M. Sze, *Physics of Semiconductor Devices* (Wiley-Interscience, New York, 1981).
[33] S. J. Breuer, Ph.D. thesis, Department of Physics, University of Newcastle Upon Tyne, 1994.
[34] A. T. Collins and A. W. Williams, J. Phys. C **4**, 1789 (1971).
[35] V. Prosser, Czech. J. Phys., Sect. A **15**, 128 (1965).
[36] P. J. Dean, E. C. Lightowlers, and D. R. Wight, Phys. Rev. **140**, A352 (1965).
[37] G. L. Pearson and J. Bardeen, Phys. Rev. **75**, 865 (1949).
[38] J. P. Lagrange, A. Deneuville, and E. Gheeraert, Diamond Relat. Mater. **7**, 1390 (1998).
[39] S. K. Estreicher and M. Sanati, Proceedings of the 23rd International Conference on Defects in Semiconductors July 24–29, 2005, Awaji Island, Japan [Physica B **376–377**, 940 (2006)].
[40] O. A. Williams, M. Nesládek, J. J. Mare, and P. Hubík, in *Physics and Applications of CVD Diamond*, edited by S. Koizumi, C. Nebel, and M. Nesladek (Wiley-VCH, Weinheim, 2008), Chap. 2, pp. 13–28.
[41] T. Teraji, in *Physics and Applications of CVD Diamond*, edited by S. Koizumi, C. Nebel, and M. Nesladek (Wiley-VCH, Weinheim, 2008), Chap. 3, pp. 29–76.
[42] R. L. Aggarwal and A. K. Ramdas, Phys. Rev. **140**, A1246 (1965).
[43] A. Nylandsted Larsen, A. Mesli, K. Bonde Nielsen, H. Kortegaard Nielsen, L. Dobaczewski, J. Adey, R. Jones, D. W. Palmer, P. R. Briddon, and S. Öberg, Phys. Rev. Lett. **97**, 106402 (2006).
[44] J. J. Xie and S. P. Chen, J. Phys. D **32**, 1252 (1999).
[45] G. D. Watkins and J. W. Corbett, Phys. Rev. **134**, A1359 (1964).
[46] For the calculated values in silicon we use a conduction-band effective mass of 0.36 m_e with six equivilent minima, and a band gap energy of 1.12 eV, taken from Ref. 32.
[47] M. G. Ganchenkova, V. A. Borodin, and R. M. Nieminen, Proceedings of the Seventh International Conference on Computer Simulation of Radiation Effects in Solids, June 28-July 2, 2004, Helsinki, Finland [Nucl. Instrum. Methods B **228**, 218 (2005)].